negative lift coefficient increases nearly linearly with the increase of the exit velocity of the RCS thruster. Negative lift coefficient is considered because the RCS thruster is located at the upper surface of the body. Other calculations are made with an angle of attack and a variation of the exit pressure of the RCS thruster. More results are given in Ref. 6.

Final Remarks

In this Note, some results for the problem of the interaction of rocket plumes with the outer hypersonic flowfield during a re-entry maneuver are presented. Also a method is shown to improve the applicability of the numerical code to expansions around corners. For the first approximation, a two-dimensional model and the Euler equations are used. But there are some concerns: if the Euler equations are valid in some regions of the flowfield. Especially in the highly viscous leeside flowfield behind the jet, the Euler equations are not valid. Another significant concern is the viscous interaction between the jet and the flowfield. Also, a boundary-layer separation would occur and the pressure pertubations from the jet propagate through the subsonic layer. All of these phenomena cannot be treated with the Euler equations. Nevertheless, this model is chosen as a first step. The first results of a calculation with the full Navier-Stokes equations show large differences in the flow pattern especially at the recirculating region.[3] Applying the Navier-Stokes equations, lift changes in the range of 5%, while drag is influenced by the order of 10% for Reynolds numbers of $Re = \mathcal{O}(10^4)$. The RCS thruster is a point source and not a line source of mass, which means that the problem is, in reality, three-dimensional and should be treated as such in the future.

References

[1]McMaster, D. L., Shang, J. S., and Golbitz, W. C., "Supersonic, Transverse Jet from a Rotating Ogive Cylinder in a Hypersonic Flow," *Journal of Spacecraft and Rockets*, Vol. 26, No. 1, 1989, pp. 24–30.

[2]Schroeder, W., and Haenel, D., "An Unfactored Implicit Scheme with Multigrid Acceleration for the Solution of the Navier-Stokes Equations," *Computers & Fluids*, Vol. 15, No. 3, 1987, pp. 313–336.

[3]Schroeder, W., and Hartmann, G., "Implicit Solutions of Three-Dimensional Viscous Hypersonic Flows," *Computers & Fluids*, Vol. 21, No. 1, 1992, pp. 109–132.

[4]Schroeder, W., and Hartmann, G., "Robust Computation of 3-D Viscous Hypersonic Flow Problems," *Notes on Numerical Fluid Mechanics*, Vol. 31, 1992, pp. 128–137.

[5]Yee, H. C., "Upwind and Symmetric Shock-Capturing Schemes," NASA TM 89464, May 1987.

[6]Karl, A., "Wechselwirkung zwischen Steuerdüsenstrahl und äußerem Strömungsfeld beim Wiedereintrittsmanöver," MBB Kommunikationssysteme und Antriebe, MBB-UK-0133-91-PUB = OTN-033087, Munich, Germany, March 1991.

Gerald T. Chrusciel
Associate Editor

Thermoviscoplastic Response of Engine-Cowl Leading Edge Subjected to an Oscillating Shock-Shock Interaction

Ajay K. Pandey*
Lockheed Engineering and Sciences Company, Hampton, Virginia 23666

Introduction

AIR-BREATHING hypersonic vehicles are subjected to intense aerodynamic heating and pressure during flight. These aerodynamic loads are severe, especially at the engine-cowl leading edges, when the vehicle forebody shock wave sweeps across and interacts with the leading-edge bow shock. An accurate prediction of the vehicle thermal and structural response is essential for proper selection of materials and design parameters.

Under these conditions, high temperature levels and thermal gradients can occur locally within the structure. At such temperature conditions, the material behavior is complex because the structure can deform inelastically. For example, under the thermal conditions considered in Ref. 1 significant inelastic material behavior consisting of both time-independent and time-dependent (creep) plastic strains is observed. Thus, the prediction of the structural response requires knowledge of nonlinear material behavior.

The thermal-structural response of engine-cowl leading edges has been the subject of various studies. Elastic response of a super "thermal" conducting leading edge subjected to intense aerodynamic heating was studied in Ref. 2. A thermal-structural elasto/plastic analysis[3] with experimental verification of a cowl lip design demonstrated that plastic effects occur and may be important. These studies did not consider the time-dependent behavior of the material, which may be significant at elevated temperature. A flux-based finite element methodology that incorporates both the time-independent and time-dependent material behavior was used to predict the thermoviscoplastic response of a leading edge subjected to stationary shock-shock interaction loading in Ref 1.

The structural analyses are, traditionally, based on elastic or elasto/plastic theory. These theories cannot accurately model the load-rate effect, cyclic material behavior, stress relaxation, etc. Since these effects are more important at elevated temperature, a unified constitutive model,[4] which includes rate-independent plastic flow, creep, stress relaxation, and temperature effects, is used in the present analysis.

The purpose of this Note is to predict the thermoviscoplastic response of a leading edge subjected to an oscillating shock-shock interaction. The governing equations, finite element formulations, evaluation of viscoplastic model, and analysis details are presented in Ref. 4.

Application: Leading-Edge Analysis

The shock-shock interaction on a scramjet cowl leading edge is shown schematically in Fig. 1. The vehicle nose bow shock interacts with the cowl bow shock resulting in a shock-shock interference pattern that impinges on the leading-edge surface. Perturbation in the flight conditions, transient structural response of the vehicle, or shock instabilities may result in the shock pattern oscillating inward and outward across the leading edge, resulting in cyclic variation of the aerothermal loads. The shock-shock interference pattern and impingement location are assumed to change with time and oscillate across the leading edge. The semicircular B1900 + Hf leading edge computational model has an external diameter of 0.25 in. and a skin thickness of 0.015 in.

Aerothermal Loads

The leading edge is subjected to highly localized aerodynamic heating due to the shock-shock interaction, which moves inward

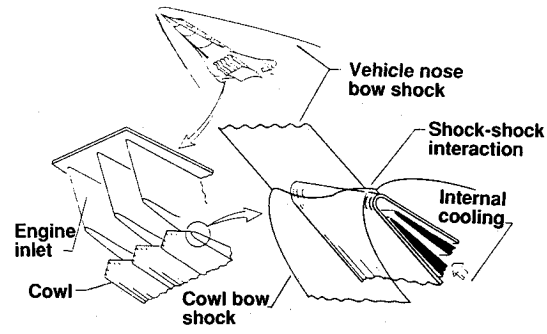

Fig. 1 Schematic diagram of shock-shock interaction on scramjet engine-cowl leading edge of an aerospace vehicle.

Received March 26, 1992; revision received Aug. 19, 1992; accepted for publication Aug. 24, 1992.

*Principal Engineer, Langley Project Officer. Member AIAA.

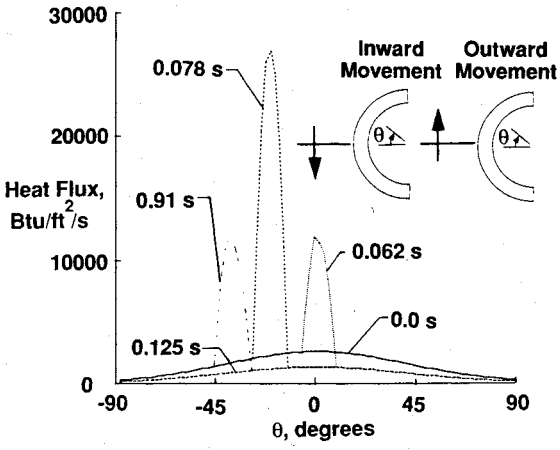

Fig. 2 Outer surface heating profiles at five typical times during the inward movement.

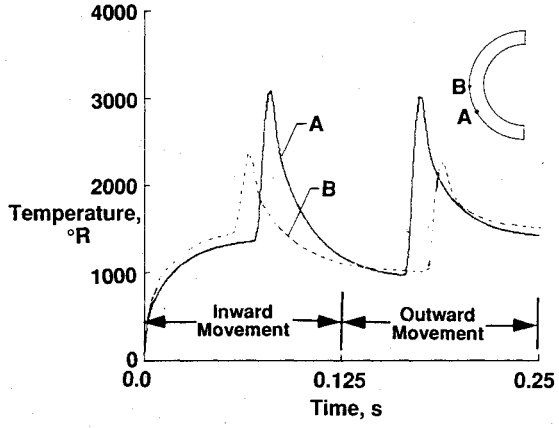

Fig. 3 Predicted temperature response at two points on the leading edge during the inward and outward movement of shock-shock interference pattern.

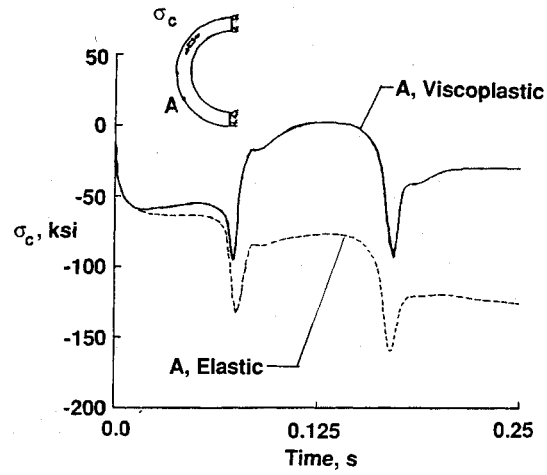

Fig. 4 Comparison of circumferential stress histories from elastic and viscoplastic analyses of the leading edge.

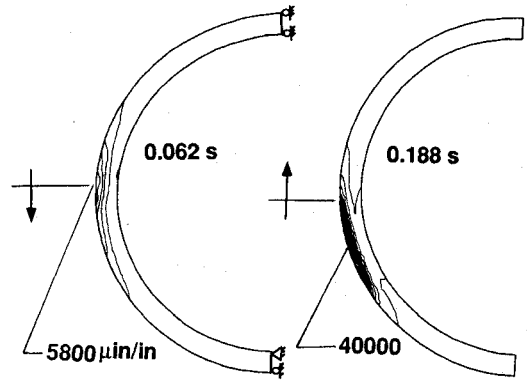

Fig. 5 Effective plastic strain contours indicating the propagation of plastic region and maximum plastic strain (in microinch/inch) for the leading edge at two selected times during the inward and outward movement.

(toward the vehicle body) and outward. The aerodynamic heating on the outer surface of the leading edge at five typical times during the inward movement is shown in Fig. 2. About 90 such profiles are used to describe the transient heating during the inward movement and the same number are used during the outward movement. During the inward movement, the shock-shock interaction reaches the centerline ($\theta = 0$ deg) at 0.062 s, however, the peak heat flux of 28,000 Btu/ft^2/s occurs at 0.078 s at $\theta = -21$ deg. Correspondingly, during the outward movement the shock reaches the peak heating location ($\theta = -21$ deg) at 0.172 s and centerline at 0.188 s. The inner surface is convectively cooled and is subjected to an internal pressure of 250 psi. The external surface emits radiant energy to space and is also subjected to aerodynamic pressure, which has the same variation as the aerodynamic heating and a peak level of 1000 psi.

Thermoviscoplastic Response

For the aerodynamic heating, shown in Fig. 2, the predicted temperature histories at two locations [points A ($\theta = -21$ deg) and B ($\theta = 0$ deg)] are presented in Fig. 3. The peak temperatures at points A and B are approximately 3100 and 2300°R, respectively. The leading edge experiences a localized high temperature region and attendant large temperature gradients through the thickness. The backside temperature is approximately 250°R.

The predicted structural temperature, external aerodynamic pressure, and coolant pressure are used to predict the viscoplastic response of the leading edge. The leading edge ends ($\theta = \pm 90$ deg) are constrained from moving in the horizontal direction but can move in the vertical direction as shown in Fig. 4. The predicted circumferential stress histories at location A, from the elastic and viscoplastic analyses, are shown in the figure. At time $t = 0$ s, the external pressure, internal pressure, external heating, and internal cooling are instantaneously applied; local bending introduces compressive stress on the outer surface and tensile stress on the inner surface. Thereafter as the shock moves inward and outward across the leading edge, the stress-time histories reflect a complex interplay between thermal stress and temperature-dependent inelastic behavior. During the inward movement, the temperature on the outer surface rises and causes increase in the compressive stresses. The material softens with a steep reduction in elastic modulus at elevated temperature. As the shock moves past the leading edge, the outer surface temperature drops to about 1000°R and the circumferential stresses are less than those predicted by elastic analysis. The outer surface experiences compressive stresses again during the outward movement and peak stresses remain at or below the saturation stress level. The stresses from the elastic analysis have similar variation but at a higher stress level. At the end of the outward movement the stress predicted by the elastic analysis is 125 ksi compared to 20 ksi predicted by the viscoplastic analysis.

A further measure of the plastic behavior was derived by calculating an effective plastic strain[1] based on the normal and shearing plastic strain components. The predicted contours of effective plastic strains at two different times during the inward and outward movement are shown in Fig. 5. Note that yielding occurs at a strain of about 2000 μin./in. at 2060°R. During the inward movement at 0.062 s, when the shock is near the centerline, a small portion of the leading edge experiences plastic strain. As the shock moves inward and outward, a significant portion of the leading edge has become plastic with a peak value of 40,000 μin./in. at 0.188 s. The plastic strains will result in permanent deformation and introduce

residual stresses after the leading-edge temperatures return to steady-state conditions.

Concluding Remarks

A finite element thermoviscoplastic analysis method, which employs a unified constitutive model, is used to predict the thermoviscoplastic response of a leading edge subjected to the heating and pressure from an oscillating shock-shock interaction. Both elastic and viscoplastic analyses of a B1900+Hf leading edge were performed. The elastic analysis tends to overestimate stresses. The viscoplastic response during the second cycle is quite different even though the applied loading was the same as the first cycle. The viscoplastic analysis provides more realistic stresses because the inelastic behavior is included. The leading edge experiences plastic strain in the high heat flux region. The predicted plastic region extends from the outer to inner surface and increases with time as the shock oscillates across the leading edge.

Acknowledgments

This research work was performed in the Aerothermal Loads Branch of NASA Langley Research Center, and was supported by Contract NAS1-19000. The author wishes to thank Allan Wieting and Pramote Dechaumphai for their valuable suggestions.

References

[1]Pandey, A. K., Dechaumphai, P., and Thornton, E. A., "Finite Element Thermoviscoplastic Analysis of Aerospace Structures," *Thermal Structures and Materials for High-Speed Flight*, edited by E. A. Thornton, Vol 140, Progress in Astronautics and Aeronautics, AIAA, Washington, DC, 1992, pp. 229–253.

[2]Dechaumphai, P., Thornton, E. A., and Wieting, A. R., "Flow-Thermal-Structural Study of Aerodynamically Heated Leading Edge," *Journal of Spacecraft and Rockets*, Vol. 26, No. 4, 1989, pp. 201–209.

[3]Melis, M. W., and Gladden, H. J., "Thermostructural Analysis with Experimental Verification in a High Heat Flux Facility of a Simulated Cowl Lip," AIAA Paper 88-2222, April 1988.

[4]Pandey, A. K., "Thermoviscoplastic Analysis of Engine Cowl Leading Edge Subjected to Oscillating Shock-Shock Interaction," AIAA Paper 92-2537, April 1992.

Earl A. Thornton
Associate Editor

Hypervelocity Stagnation-Point Heating Rate Discrepancies

Ernest V. Zoby* and Roop N. Gupta*
NASA Langley Research Center, Hampton, Virginia 23681
and
Kam-Pui Lee†
ViGYAN, Inc., Hampton, Virginia 23665

Introduction

PROPOSED Earth entry velocities for space exploration vehicles are typically in the range of 12–16 km/s. These high-energy flowfields result in very large radiative and convective surface heat fluxes. An earlier investigation[1] had scoped the magnitude of these fluxes for several velocities as well as for candidate thermal protection systems. The calculations of Ref. 1 were based on a variable Lewis number with a binary diffusion coefficient computed for molecular nitrogen and atomic oxygen. The selection of a dominant species for the binary diffusion assumption has also been employed in Martian entry[2] and in aerobrake[3] analyses. This species combination of molecular nitrogen and atomic oxygen for a binary diffusion calculation would seem to be appropriate for at least the inner flowfield regions since these are the dominant species.

However, for the velocities previously noted, the choice of molecular nitrogen and atomic oxygen as the dominant pair for binary diffusion through the shock layer is not appropriate. At the very high temperatures that characterize the majority of the flowfield for these hypervelocity conditions, molecular nitrogen is either not present or is present only as a trace species. As a result, a computational study was conducted to assess the influence of different methods of implementing the Lewis number in flowfield calculations on the heat transfer. For this study, the calculations were based on several freestream velocities and wall temperature assumptions. Since significant differences were noted in the convective heating predictions, the purpose of this Note is to highlight these results and offer some related observations.

Computational Procedure

The viscous shock-layer (VSL) method of Ref. 1 was used to compute the flowfields for the present study. For brevity, the basic equations and boundary conditions are not presented herein but are the same as those used in Ref. 1. For this study, the calculations are based on an equilibrium-air assumption for the flowfield chemistry and do not include radiation effects. The thermodynamic and transport properties are based on the investigation of Ref. 4

Discussion of Results and Conclusions

Stagnation-point convective heating calculations were performed at 70-km altitude for a nose radius of 3.05 m and the freestream velocities and wall temperatures shown in Table 1. The first temperature value for each velocity is the radiative equilibrium wall temperature for the variable Lewis number case. The heating rates and associated ratios are computed for three calculations of the Lewis number. One of these calculations is for a variable Lewis number computed through the shock layer. The related binary diffusion coefficient calculation is based on the assumption that molecular nitrogen and atomic oxygen are the dominant species. The surface Lewis number, which is computed with the radiative equilibrium

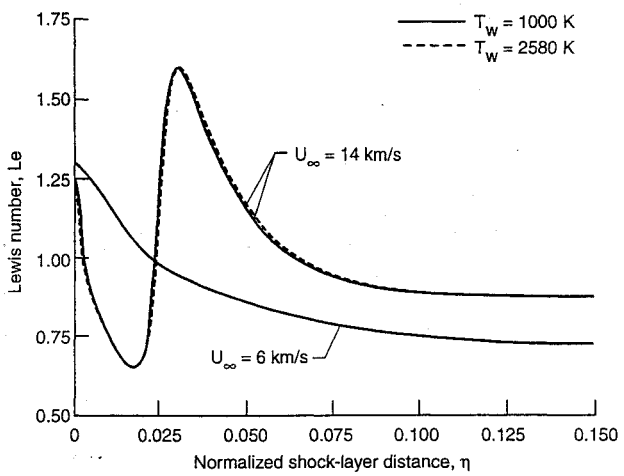

Fig. 1 Shock-layer Lewis number distribution for different freestream velocities and wall temperatures.

Received March 4, 1993; revision received March 18, 1993; accepted for publication March 18, 1993.

*Research Engineer, Aerothermodynamics Branch, Space Systems Division. Associate Fellow AIAA.

†Research Engineer. Member AIAA.